FERMILAB-CONF-76-121-E

E-88
Conf. on High Energy Physics
Tbilisi, USSR

Diffractive Production of Rho Mesons by 150 GeV Muons

H.L. Anderson, V.K. Bharadwaj, N.E. Booth, R.M. Fine, W.R. Francis, B.A. Gordon, R.H. Heisterberg, R.G. Hicks, T.B.W. Kirk, G.I. Kirkbride, W.A. Loomis, H.S. Matis, L.W. Mo, L.C. Myrianthopoulos, F.M. Pipkin, S.H. Pordes, T.W. Quirk, W.D. Shambroom, A. Skuja, L.J. Verhey, W.S.C. Williams Richard Wilson and S.C. Wright

Enrico Fermi Institute and Department of Physics, The University of Chicago, Chicago, Illinois 60637, and Department of Physics, Harvard University, Cambridge, Massachusetts 02138, and Department of Physics, The University of Illinois, at Urbana-Champaign, Urbana, Illinois 61801, and Nuclear Physics Laboratory, The University of Oxford, Oxford, OX1 3RH, England

ABSTRACT

Cross sections for diffractive rho muo-production in hydrogen are presented for $90 < \nu < 135$ GeV and $Q^2 < 5$ $(GeV/c)^2$. The results are compared with lower energy data and the predictions of simple vector dominance models.

*Work supported by the National Science Foundation under Contract No. MPS 71-03-186, by the U.S. Energy Research and Development Administration under Contract Nos. AT (11-1)-3064 and 1195, and by the Science Research Council (United Kingdom).

We have extended the study of rho meson lepto-production to higher energies. The experiment was performed at the Fermi National Accelerator Laboratory as part of a comprehensive program of muon scattering using the spectrometer constructed by this group. Details of the apparatus have been described in previous letters.[1] 150 GeV positive muons were incident upon a 1.19 meter liquid hydrogen target. The experiment trigger required that a muon leave the beam either by scattering through a large angle ($\gtrsim$ 14 mr) or/ and by suffering a large energy loss ($\gtrsim$ 90 GeV). In this paper data are reported for which $90 < \nu < 135$ GeV and $Q^2_{min} < Q^2 < 5.0$ $(GeV/c)^2$, where ν is the energy lost by the scattered muon, Q^2 is the square of the muon four-momentum transfer, and Q^2_{min} is the minimum kinematically allowed value of Q^2 at a given ν.

2.17×10^{10} incident muons yielded 150K triggers. Events in which a scattered muon was reconstructed were examined for evidence of the production of hadronic pairs. Since the recoil proton was detected in only a small fraction of the events, the selection criteria required that

1) one positive and one negative particle be observed in addition to the scattered muon,
2) the production vertex occur within the target fiducial volume, and
3) the measured momenta reconstruct the energy of the incident muon within 3.0 GeV (σ_{RMS} = 1.1 GeV.)

The invariant mass of these elastic, neutral pairs was calculated assuming that both particles were pions. This sample contained a large number ($\sim$ 70%) of low mass (< 0.5 GeV), electron-positron pairs from purely electromagnetic processes. These were identified by observing their cascade showers behind a 3 r.l. steel radiator. Since pions could also generate such showers, a clean separation of events was achieved by demanding

4) a pair opening angle greater than 5.0 mr. (σ_{RMS} = 0.6 mr.)

Polynomial fits to the background outside the energy balance cut (3) indicated a 16% contamination due to hadronic pairs with one or more undetected, slow pions. This background was reduced to 3 ± 2%, independent of Q^2 and ν, by requiring that

5) the four-momentum transfer squared to the proton at the production vertex, t, satisfy $|t| < 0.6$ (GeV/c)^2. ($\sigma_{RMS} \approx \sqrt{t}/8$ GeV/c)

The resulting sample of hadron pairs contained 184 events. These data were grouped into Q^2 and ν bins (Table 1), and corrected for beam reconstruction losses (24%), pion absorption (6.5%/pion), chamber inefficiencies (7.0%/particle), reconstruction inefficiencies for tracks close to the beam (between 0 and 46%; 5% average), trigger inefficiencies (between 2 and 12%; average 7%), multiple scattering and resolution smearing (between 1 and 8%; average 3%), and geometric acceptance. Since insufficient empty target dipion data were available for a simple subtraction, a 5% correction factor was employed to remove the contribution from the target vessel. The total systematic uncertainty is estimated at 7%.

Table 1 Bin Kinematics

Q^2 (GeV/c)^2	$\langle Q^2 \rangle$ (GeV/c)^2	$\langle \nu \rangle$ (GeV)	$\langle \varepsilon \rangle$
0.01-0.10	.05	98	0.55
0.02-0.10	.07	121	0.39
0.1 -0.3	.16	104	0.55
0.1 -0.3	.16	124	0.38
0.3 -1.0	.62	112	0.48
1.0 -5.0	2.2	112	0.50

Dividing by the usual virtual photon flux factor,[2] we derive cross sections $d\sigma/dmdt\ (Q^2,\nu,m,t)$ for the reaction $\gamma_{virtual} + p \rightarrow \pi^+ + \pi^- + p$. Here m is the dipion mass. Radiative corrections were applied following the general formalism of Bartl and Urban.[3] These increased the observed cross section by an average of 3% at $Q^2 = .05$; 8% at $Q^2 = 2.5(GeV/c)^2$. In each Q^2, ν bin the cross section was integrated over t. The prescription of Yennie[4] was employed in fitting the resulting mass spectra. A p-wave, Breit-Wigner rho was allowed to interfere with a diffractive, but nonresonant, dipion background. The rho mass and width were fixed throughout at 0.77 and 0.15 GeV respectively. The spectra were fit in the mass interval 0.4 to 1.1 GeV to the following form as smeared by the calculated resolution

$$\frac{d\sigma}{dm} = \frac{C_1\, m m_\rho \Gamma}{(m_\rho^2 - m^2)^2 + m_\rho^2\Gamma^2} \left\{ 1 + C_2 \left(\frac{m_\rho^2 - m^2}{m^2} \right) + C_3 \left(\frac{m_\rho^2 - m^2}{m^2} \right)^2 \right\}$$

where $$\Gamma = \Gamma_\rho \frac{m_\rho}{m} \left(\frac{m^2 - 4m_\pi^2}{m_\rho^2 - 4m_\pi^2} \right)^{3/2}$$

and the C's are the free parameters of the fit. The results of the fits were used to obtain cross sections for the process $\gamma_{virtual} + p \rightarrow \rho + p$. Figure 1 presents the unsmeared mass spectra and fits.

Photoproduction cross sections were extrapolated from the measurements below $Q^2 = 0.3\ (GeV/c)^2$ assuming $\sigma_\rho(Q^2) = \sigma_\rho(0)(1 + Q^2/m_\rho^2)^{-2}$. Figure 2 compares these results with representative lower energy data. The curve is the quark model prediction relating this process to elastic pion scattering via VDM[5] calculated using the colliding beam value for the rho-photon coupling constant. Although the data exhibit no significant energy dependence within our kinematic range, the real photon production cross section falls from about 20 μb at $s = 5\ GeV^2$ to 7.9 ± 0.8 μb near $s = 200\ GeV^2$. The observed decrease agrees well in both shape and magnitude with this model. A much better fit is obtained with $\gamma_\rho^2/4_\pi = 0.72$ indicating a mild dependence of the coupling constant on the photon mass.

Figure 3 displays the Q^2-dependence of the observed production cross section, averaged over ν, along with low energy data from Cornell.[6] Once the s-dependence of the real photon cross section is removed, the data are remarkably energy independent and fit quite well the same rho propagator squared form factor of naive vector dominance[7] used in the photoproduction extrapolation.

The t-distributions were fit to a simple exponential normalized to the observed production cross section, $(\sigma_\rho b)\exp(bt)$. Figure 4 displays these data and fits for various Q^2 bins. The data suggest a broadening with increasing Q^2 but are also consistent with a single slope parameter $b = 7.3 \pm 0.7\ (\mathrm{GeV/c})^{-2}$. The distribution at high Q^2 appears flatter, but, being based on only 11 events, the uncertainty is large. Preliminary analysis of deuterium data in this same kinematic region does not support this high Q^2 effect. Nieh[8] has used a vector dominance model to predict that there will be no flattening of the t-distribution for $Q^2 < 20(\mathrm{GeV/c})^2$ at the energies of this experiment.

The angular distribution of the decay pions has been studied, yielding information on the spin structure of the production process. Since the polarization parameter ε, of the virtual photon beam is not large in this kinematic region (Table 1), the effects are not dramatic. Assuming s-channel helicity conservation and dominance of natural parity exchange, the data were fit to[9]

$$W(\cos\theta,\psi) = \frac{1}{1+\varepsilon R_\rho}\ \frac{3}{8\pi}\ \{\sin^2\theta(1 + \varepsilon\cos 2\psi) + 2\varepsilon R_\rho\cos^2\theta$$

$$- \sqrt{2\varepsilon(1+\varepsilon)R_\rho}\ \cos\delta\sin 2\theta\cos\psi$$

$$+ \sqrt{2\varepsilon(1-\varepsilon)R_\rho}\ P\ \sin\delta\sin 2\theta\sin\psi\}$$

where R_ρ is the ratio of the longitudinal to the transverse rho production cross section, δ is the phase difference between the longitudinal and the

transverse amplitudes, and P is the muon beam polarization ($\sim$ 0.7). Here θ is the polar angle of the π^+ in the rho rest frame with z-axis opposite to the direction of the recoil proton and ψ is the azimuthal angle of the π^+ referenced to the muon scattering plane.

Figure 5 displays the data for several Q^2 bins. The results of the fits are presented in Table 2. In contrast to the low energy ($s < 4$ GeV^2) data from DESY [10], the situation at high energy exhibits mild Q^2 dependence. R_ρ remains small as Q^2 increases to 1.0(GeV/c)^2. The phase difference is consistent with zero everywhere measured.

Table 2 SCHC Fit Results

$\langle Q^2 \rangle$(GeV/c)^2	$\langle \varepsilon \rangle$	R_ρ	δ(degrees)
0.05	0.55	0.1±0.1	-18±90
0.07	0.39	$0.0^{+0.05}_{-0}$	---
0.16	0.55	0.3±0.2	10±80
0.16	0.38	$0.0^{+0.04}_{-0}$	---
0.59	0.33	$0.1^{+0.1}_{-0.05}$	30±70
0.67	0.52	0.7±0.4	0±60

We thank the staffs of Fermilab, of our home institutions, and of the Rutherford lab whose help made this work possible. We gratefully acknowledge numerous discussions with and suggestions by Dr. Garland Grammer on the subject of radiation corrections.

LIST OF FIGURES

References

1. W. A. Loomis, et. al., Phys. Rev. Lett. 35, 1483 (1975).
2. L. N. Hand, Phys. Rev. 129, 1834 (1964).
3. A. Bartl and P. Urban, Acta Phys. Avst. 24, 139 (1966).
4. R. Spital and D. R. Yennie, Phys. Rev. D9, 126 (1974).
5. H. Joos, Phys. Lett. 24B, 103 (1967)
6. L. Ahrens, et. al., Phys. Rev. Lett. 31, 131 (1973); Phys. Rev. D9, 1894 (1974).
7. J. J. Sakurai and D. Schildknecht, Phys. Lett. 40B, 121 (1972).
8. H. T. Nieh, Phys. Lett. 38B, 100 (1972). See also H. Cheng and T. T. Wu, Phys. Rev. 183, 1324 (1969) and J. D. Bjorken, J. B. Kogut, and D. E. Soper, Phys. Rev. D3, 1382 (1971).
9. K. Schilling and G. Wolf, Nucl. Phys. B61, 381 (1973).
10. P. Joos, et. al., data presented in the review by G. Wolf, in Proceedings of the 1975 International Symposium on Lepton and Photon Interactions at High Energies, edited by W. T. Kirk (Stanford University, Stanford, California, 1976).

Yennie Fits

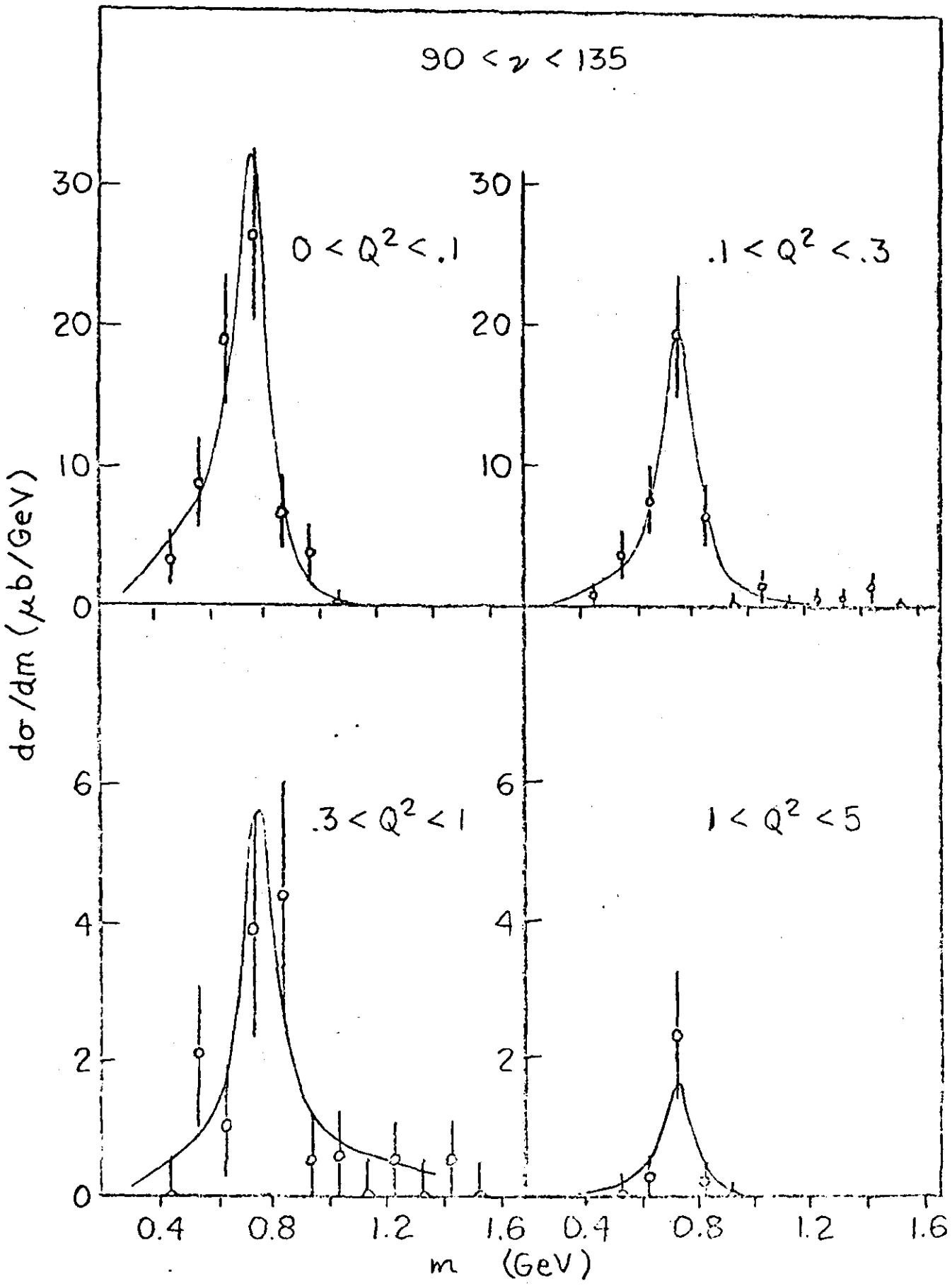
90 < ν < 135
0 < Q² < .1
.1 < Q² < .3
.3 < Q² < 1
1 < Q² < 5
dσ/dm (μb/GeV)
m (GeV)
0
10
20
30
2
4
6
0.4
0.8
1.2
1.6

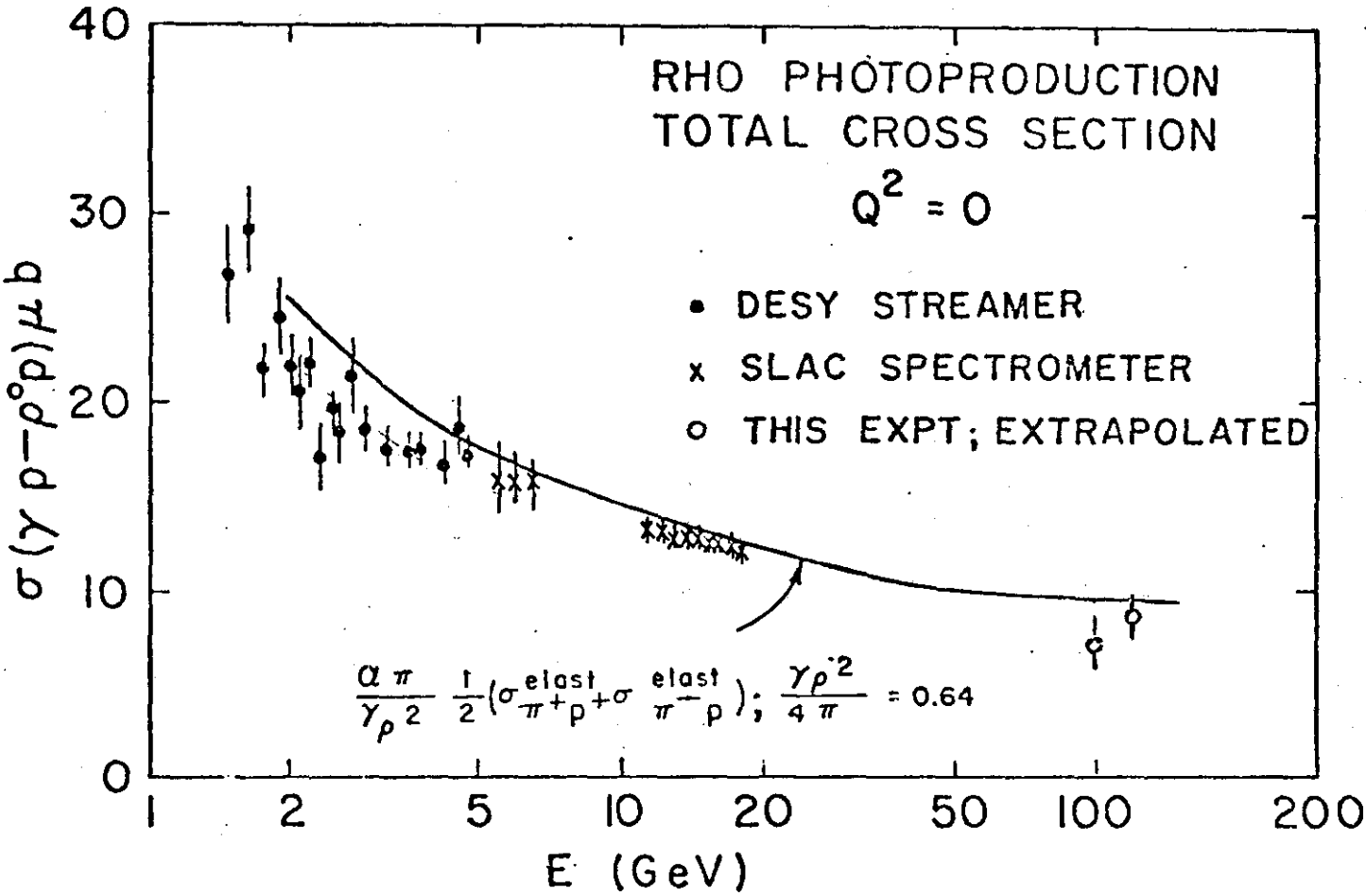
RHO PHOTOPRODUCTION
TOTAL CROSS SECTION
$Q^2 = 0$
• DESY STREAMER
x SLAC SPECTROMETER
o THIS EXPT; EXTRAPOLATED
$\frac{\alpha\pi}{\gamma_\rho^2}\frac{1}{2}(\sigma^{elast}_{\pi^+p}+\sigma^{elast}_{\pi^-p})$; $\frac{\gamma_\rho^2}{4\pi} = 0.64$
$\sigma(\gamma p \to \rho^0 p)\mu b$
E (GeV)
0
10
20
30
40
1
2
5
10
20
50
100
200

Fig. 2

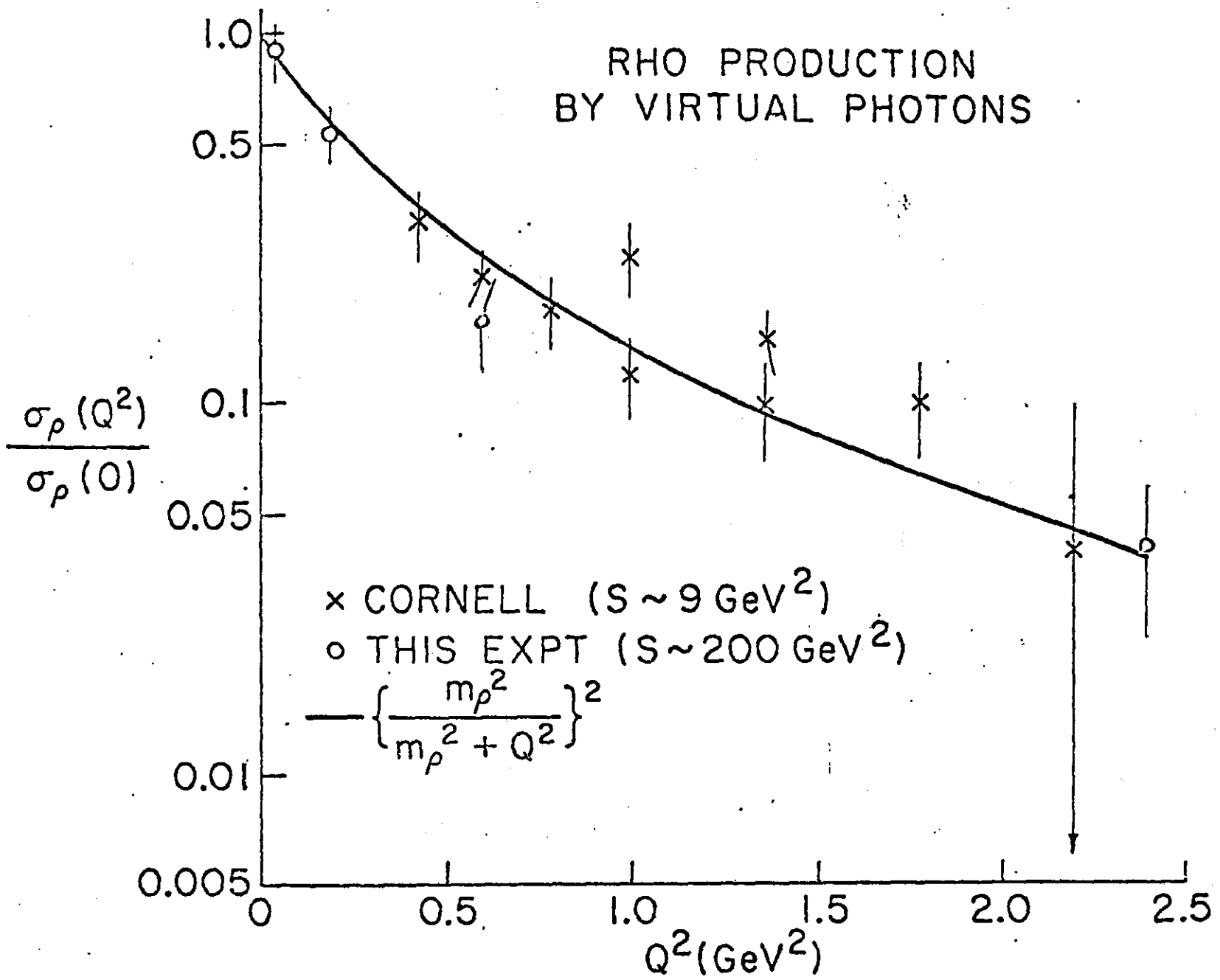
RHO PRODUCTION
BY VIRTUAL PHOTONS
$\frac{\sigma_\rho(Q^2)}{\sigma_\rho(0)}$
1.0
0.5
0.1
0.05
0.01
0.005
0
0.5
1.0
1.5
2.0
2.5
$Q^2(GeV^2)$
× CORNELL ($S \sim 9\ GeV^2$)
o THIS EXPT ($S \sim 200\ GeV^2$)
$\left\{\frac{m_\rho^2}{m_\rho^2 + Q^2}\right\}^2$

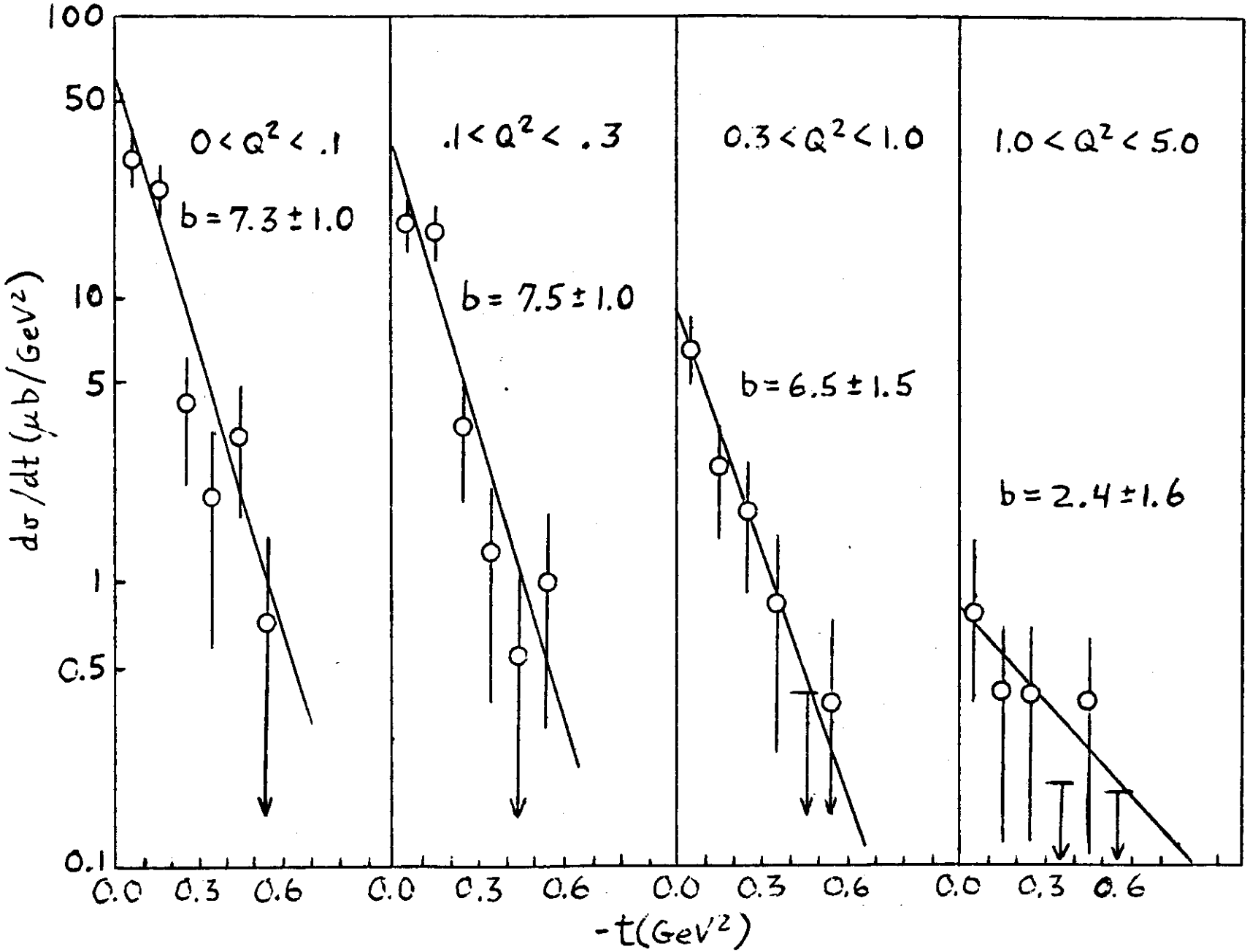
100
50
10
5
1
0.5
0.1
dσ/dt (μb/GeV²)
0 < Q² < .1
b = 7.3 ± 1.0
.1 < Q² < .3
b = 7.5 ± 1.0
0.3 < Q² < 1.0
b = 6.5 ± 1.5
1.0 < Q² < 5.0
b = 2.4 ± 1.6
0.0
0.3
0.6
-t(GeV²)

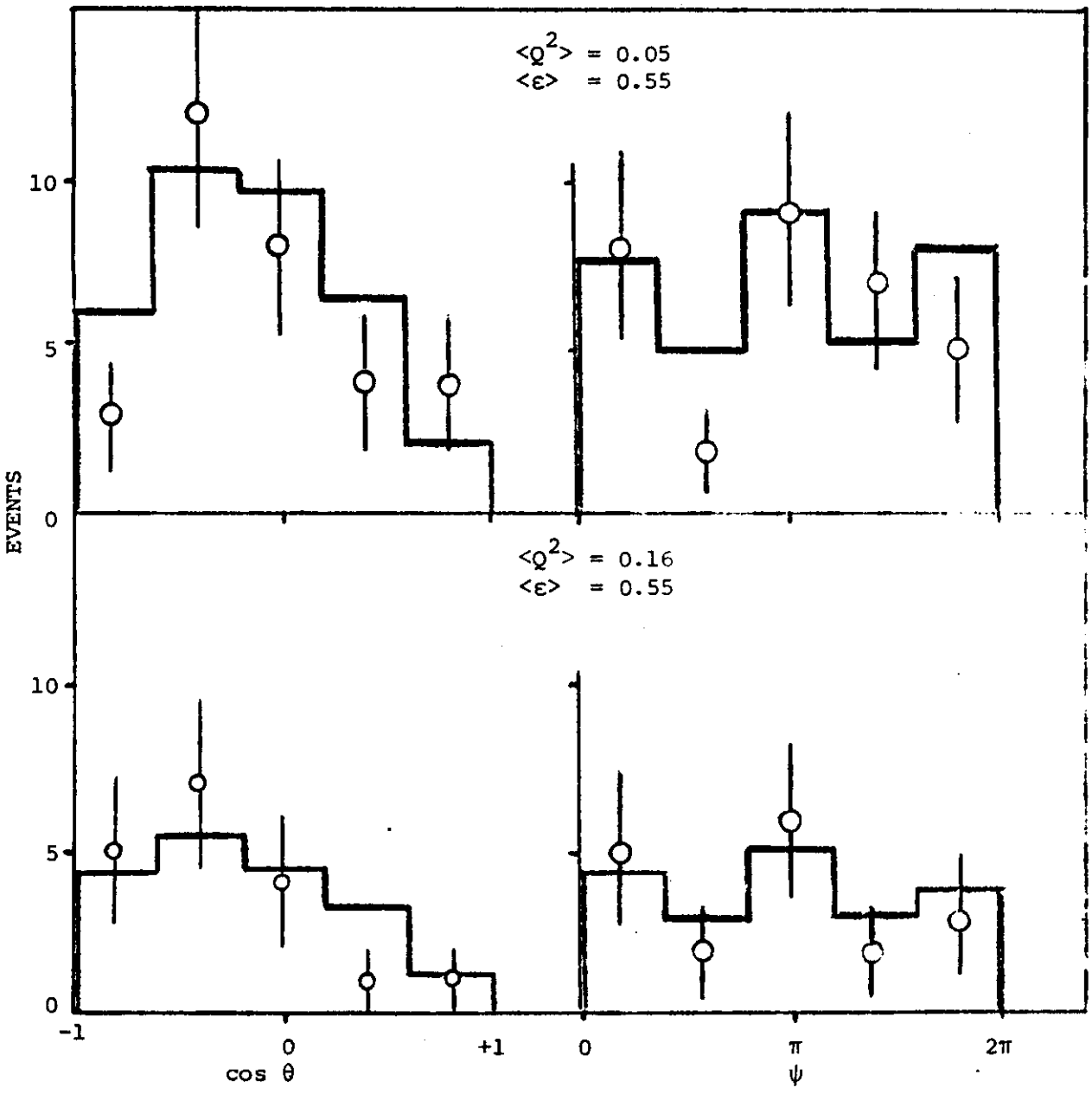

Fig. 5